J Mater Sci: Mater Electron (2007) 18:487–493
DOI 10.1007/s10854-006-9064-9

Properties of brush plated CdS films

K. R. Murali · S. Kumaresan · J. Joseph Prince

Received: 26 April 2006 / Accepted: 19 October 2006 / Published online: 23 November 2006

Abstract Cadmium sulphide (CdS) thin films were deposited for the first time using the brush plating technique from the precursors on titanium and conducting glass substrates. The films were polycrystalline possessing single-phase hexagonal structure. Surface morphological studies indicated increase of grain size with increase of post deposition temperature. Optical band gap of 2.39 eV was obtained. XPS studies indicated the formation of CdS. Photo electrochemical cell studies indicated higher current and voltages compared to earlier reports on thin film electrodes. Mott–Schottky studies exhibited n-type behaviour with a carrier density of 10^{18} cm^{-3}. Spectral response measurements indicated a quantum efficiency of 0.35.

1 Introduction

Extensive research has been done on the deposition and characterization of cadmium sulphide (CdS) semiconducting thin films due to their potential application in the area of electronic and optoelectronic device [1, 2]. Polycrystalline CdS thin films are generally used in $CuInSe_2$ (CIS) and CdTe solar cells, as a window material for transmitting the light absorbed by CIS or CdTe and also as the n-type material for p–n junction of the solar cells [3]. This material has been prepared by several methods including evaporation [4], sputtering [5], electrodeposition [6] and spray [7], Chemical bath deposition [8]. In this investigation CdS films have been deposited for the first time using the brush plating technique.

K. R. Murali (✉)
Electrochemical Materials Science Division, Central Electrochemical Research Institute, Karaikudi 630 006, India
e-mail: muraliramkrish@gmail.com

S. Kumaresan
Department of Physics, Saranathan College of Engineering, Trichy, India

J. J. Prince
Department of Physics, Bharathidasan School of Engineering and Technology, Trichy, India

2 Experimental methods

CdS films were prepared on conducting glass and titanium substrates using selective plating technique. The precursors used for the deposition of CdS were 0.5 M $CdSO_4$, 0.1 M sodium thiosulphate (Both precursors were of AR grade and E. Merck (Germany) make) and triply distilled water to make up the solution to 10 ml. The cotton wrapped graphite anode was dipped in the precursor mixture and brushed on the stainless steel substrates. The films were deposited at a current density of 80 mA cm^{-2} at 90 °C. The deposition current density was fixed based on our earlier experience with brush-plated films [9]. It took 20 min to deposit a film of thickness 5.0 μm (thickness estimated from gravimetry). These layers were heat treated at different temperatures in the range 450–550 °C in argon atmosphere for 20 min. The films were characterized by X-ray diffraction, using Phillips X-ray diffraction unit. Optical absorption measurements were made on the films deposited on conducting glass substrates using a U3400 Hitachi UV-VIS-NIR

spectrophotometer. Surface morphology of the films were studied by JOEL 35CF SEM. Photo electrochemical Measurements were made using an ORIEL 250W Tungsten Halogen lamp.

3 Results and discussion

X-ray diffraction (XRD) patterns of cadmium sulphide films post-heat treated at different temperatures in the range 450–550°C are shown in Fig. 1. Peaks corresponding to the hexagonal phase were observed. As the heat treatment temperature increases, the crystallinity of the films also increased as evidenced by the sharpness of the XRD peaks. Peaks corresponding to (100), (002), (101), (102), (110), (103) and (112) reflections were observed. The lattice parameters were calculated from the XRD data and are found to bea = 4.145°A, c = 6.752°A, which are found to be in close agreement with the ASTM data. The crystallite size calculated using the Debye Scherrer equation is indicated in Table 1.

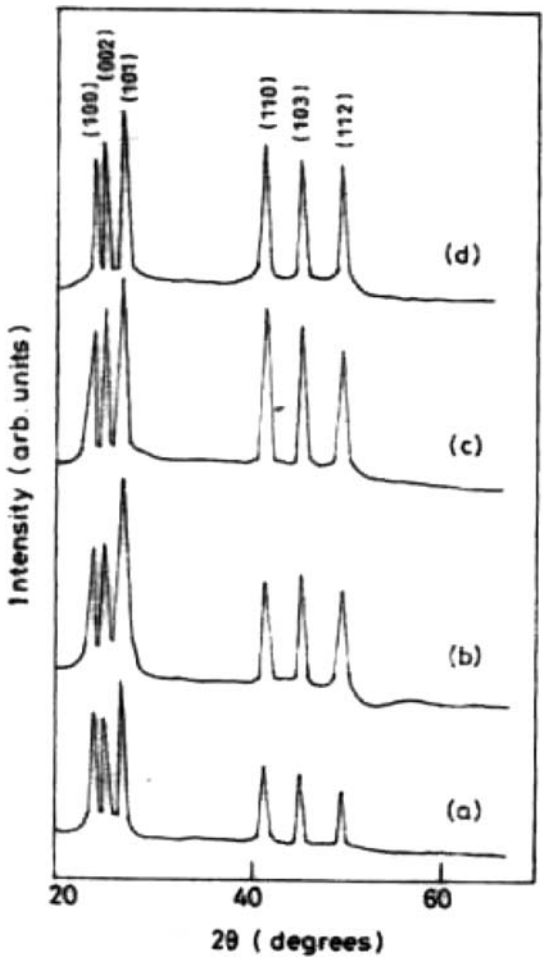

Fig. 1 XRD patterns of CdS films annealed in argon atmosphere at different temperatures (**a**) 450 °C (**b**) 500 °C (**c**) 525 °C (**d**) 550 °C

Table 1 Crystallite size of the films

Annealing temperature (°C)	Crystallite size (nm)
450	120
475	170
525	270
550	650

EDAX studies indicated the composition of the films to be Cd(64.1%) and S(35.9%), after heating at 550 °C, the concentration varied slightly as Cd(65.3%) and S(34.7%).

Fig. 2 shows the binding energies of the Cd($3d_{5/2}$ and $3d_{3/2}$) and S($3d_{5/2}$ and $3d_{3/2}$) levels of the CdS films annealed at different temperatures. There is no preferential removal of Cd on annealing, but a small amount of S is lost by evaporation. This is also evidenced from the EDAX results. As shown in the Fig. 3, the peak energy levels associated with the Cd($3d_{5/2}$ and $3d_{3/2}$) appeared at 405 and 411.7 eV respectively, these values are in close agreement with the literature values. The figure also shows the binding energies of S($3d_{5/2}$ and $3d_{3/2}$) levels at 168.0 eV and 173.0 eV respectively. The Sulphur binding energies are found to shift to lower energy values after annealing due to a small loss of S by evaporation. There is no evidence of shifting of the energy levels to higher binding energies corresponding to the oxidation of sulphur or cadmium after annealing. Atomic concentration measurements made on the annealed samples yielded an apparent Cd/S ratio of 1.62, this calculation is based on the consideration of the area sensitivity factors for Cd and S and agrees very well with the composition estimated by EDAX measurements. Depth profile study wascarried out at a sputter rate of 10 nm/min, which indicated a uniform distribution of Cd and S throughout the entire thickness.

Optical absorption measurements were made on the CdS films deposited on conducting glass substrates. Substrate absorption, if any was corrected by placing an uncoated conducting glass substrate in the reference beam. Fig. 3 shows the $(\alpha h\nu)^2$ versus $h\nu$ plot of the CdS films annealed at 550 °C. The energy gap obtained from the wavelength at which onset of maximum absorption is obtained corresponds to 2.39 eV. This value is similar to the value obtained on thin film CdS [10].

The conduction mechanism in semiconductors can be understood by analyzing the current–voltage plots. For single carrier injection at low voltages, the plot is

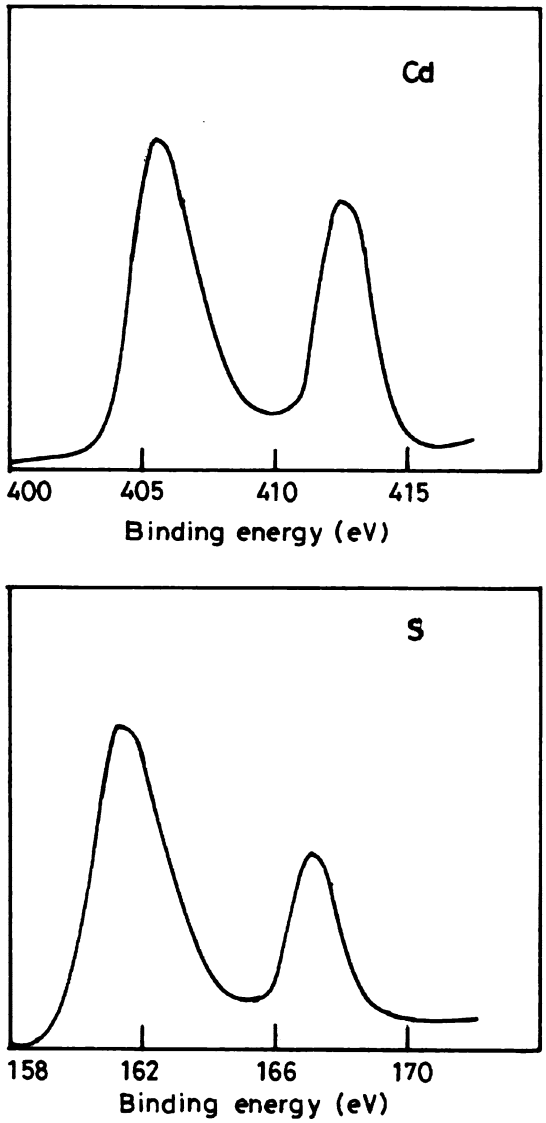

Fig. 2 XPS spectrum of Cd and S for CdS films heated at 550 °C

generally a straight line showing the validity of Ohm's law. However, at higher voltages, some deviation is expected. The I-V characteristics of the films are shown in Fig. 4. From the figure, it is understood that the plots follow a relation of the form $I \propto V^n$. The films exhibit linear characteristics up to the applied bias of 240 V. Beyond this particular voltage, the current increases sharply. This explained by noting that the current transport in the semiconductor is controlled by space charge and the current is said to be space charge limited.

The linear behaviour observed up to 240 V is attributed to the filling up of a discrete set of traps lying below or at the Fermi level. Further it is observed that for a small increase in voltage after the critical voltage (V_{TFL}) voltage at trap filled level is 240 V, the

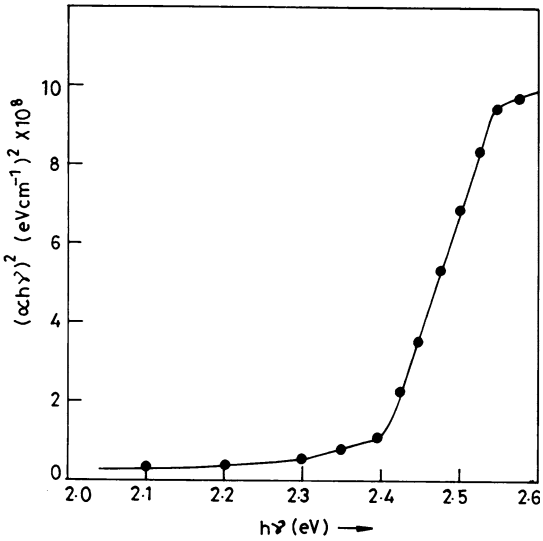

Fig. 3 $(\alpha h\nu)^2$ vs. hν plot of the CdS films annealed at 550 °C

current shoots up. This could be explained by arguing that the traps are directly filled by the charge carriers upto V_{TFL}. When the voltage reaches V_{TFL}, all the traps are filled and further increase in voltage causes a rapid increase in current. Lampert et al [11] have shown that V_{TFL} is related to the trap density N_t by the relation, $N_t = 1.1 \times 10^6 \times \varepsilon \times V_{TFL}/l^2$, where l is the film thickness and t is the relative dielectric constant of

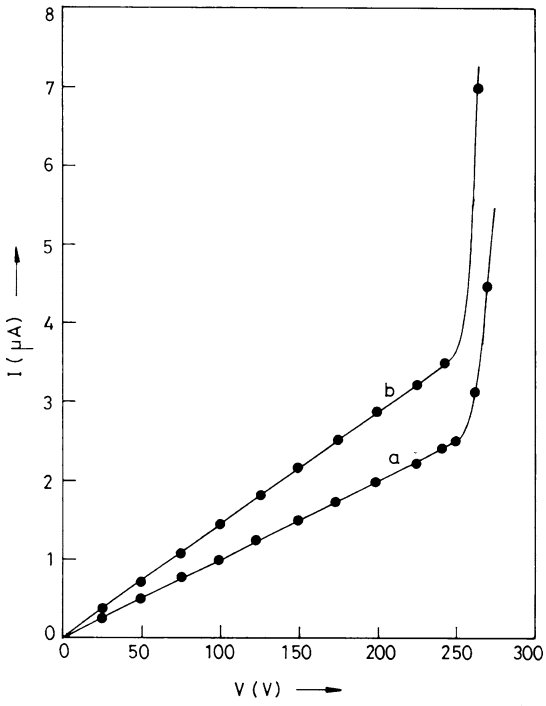

Fig. 4 Current voltage characteristics of CdS films heat-treated in argon at (**a**) 500 °C (**b**) 550 °C

the material. The trap density for both the undoped and doped films was found to be of the order of 10^{17} cm^{-3}. Similar observations have been noticed by Murali et al [12], Rooz et al [13] for electrodeposited CdSe films. Also Smith et al [14] observed similar results in the case of CdS single crystals. At sufficiently high voltages, above 240 V, the current is no longer linear and shoots up very sharply. This is consistent with the argument that the behaviour is either Ohmic or space charge limited depending on whether the volume generated carrier density or the injected carrier density predominates. The sudden increase in voltage causes the sharp increase of current to very high values. This implies that the increase in voltage forces a corresponding increase of charge in the conduction band.

Photo electrochemical (PEC) cells were prepared using the films deposited on titanium substrates heat-treated at different temperatures. The films were lacquered with polystyrene in order to stop off the metal substrate portions from being exposed to the redox electrolyte. These films were used as the working electrode. The electrolyte was 1 M polysulphide. This electrolyte was chosen, as it is well known that CdS electrode has reasonable stability and yield respectable outputs ion polysulphide. The light source used for illumination was an ORIEL 250 W tungsten halogen lamp. A water filter was introduced between the light source and the PEC cell to cut off the IR portion. The intensity of illumination was measured with a CEL suryamapi (It is an instrument manufactured by Central Electronics Limited, India used for measuring the light intensity falling on the cell) whose readings are directly calibrated in mW cm^{-2}. The intensity of illumination was varied changing the distance between the source and the cell. The power output characteristics of the cells were measured by connecting the resistance box and an ammeter in series; the voltage output was measured across the load resistance. The photocurrent as well as dark current was measured with a HIL digital multimeter. The output voltage was measured by a HIL digital multimeter.

The CdS photo electrodes were dipped in the electrolyte and allowed to attain equilibrium under dark conditions for about 10 min. The dark current and voltage values were noted. The cells were then illuminated by the light source and the current and voltage were measured for each setting of the resistance box. The photocurrent and photo voltage were calculated as the difference between the current and voltage under illumination and the dark current and voltage respectively.

The power output characteristics of the PEC cells made using the photo electrodes heat treated at different temperatures is shown in Fig. 5. From the figure, it is observed that the PEC output parameters, viz., open circuit voltage and short circuit current were found to increase for the electrodes heat treated up to a temperature of 500°C. Photo electrodes heat-treated at temperatures greater than this value exhibited lower open circuit voltage and short circuit current due to the reduction in thickness of the films as well as the slight change in stoichiometry, hence further studies were made only on the films heat treated at 500°C.

The power output characteristics of the electrodes heat treated at 500°C were studied at different intensities of illumination in the range 20–100 mW cm^{-2}. It was observed that both V_{oc} and J_{sc} increased with increase of intensity (Fig. 6). V_{oc} increased from 0.33 V to 0.50 V as the intensity increased from 20–100 mW cm^{-2}. Beyond 80 mW cm^{-2} illumination, V_{oc} was found to saturate as is commonly observed in the case of photovoltaic cells and PEC cells [15], J_{sc} is found to increase with intensity of illumination.

It is observed that the J_{sc} increases from 3.0 mA cm^{-2} to 5.0 mA cm^{-2} as the intensity increased from 20–100 mW cm^{-2}. A plot of $\ln J_{sc}$ versus V_{oc} (Fig. 7) yielded a straight line. Extrapolation of the line to the y-axis yields a J_0 value of 1.5×10^{-7} A cm^{-2}, the ideality factor (n) was calculated from the slope of the straight line and it was found to be 2.5. The effect of photo etching on the PEC performance was studied by shorting the photo electrode and the graphite counter electrode under an illumination of 100 mW cm^{-2} in 1:100 HCl for different durations in the range 0–100 s. Both photocurrent and photo voltage are found to

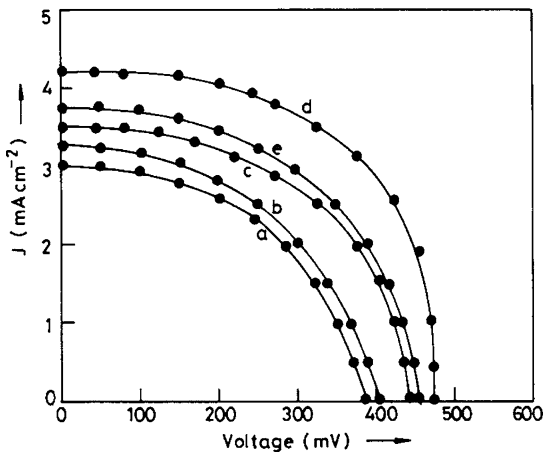

Fig. 5 Power output characteristics of CdS photo electrodes heat-treated in argon at different temperatures (**a**) 450 °C (**b**) 475 °C (**c**) 500 °C (**d**) 525 °C (**e**) 550 °C

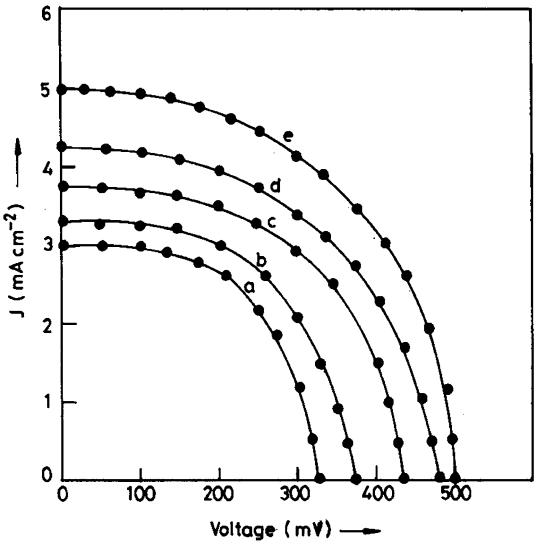

Fig. 6 Power output characteristics of CdS photoelctrodes heat-treated in argon at 500 °C and illuminated at different intensities (**a**) 20 Mw cm^{-2} (**b**) 40 mW cm^{-2} (**c**) 60 mW cm^{-2} (**d**) 80 mW cm^{-2} (**e**) 100 mW cm^{-2}

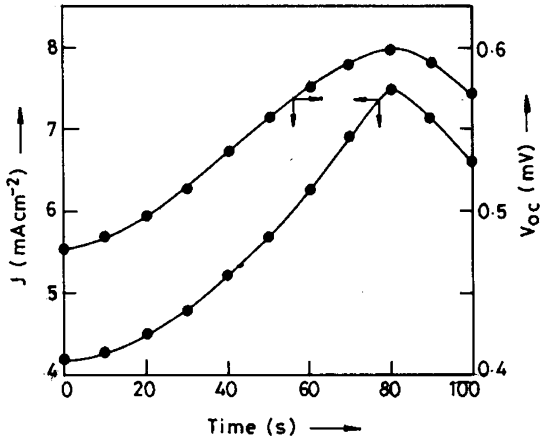

Fig. 8 Effect of photo etching on V_{oc} and J_{sc} of CdS photo electrodes heat-treated n argon at 500 °C

increase up to 80 s photo etch, beyond which they begin to decrease (Fig. 8). Photo etching leads to selective attack of surface states not accessible to chemical etchants. It is observed that during photo etching, the open circuit voltage and short circuit current increase from 0.475 V to 0.60 V and from 4.20 mA cm^{-2} to 7.50 mA cm^{-2} respectively for an intensity of 80 mW cm^{-2}. The decrease in the voltage and current beyond 80 s photo etching can be attributed to increase in surface area due to prolonged photo etching [16]. The power output characteristics (Fig. 9) after 80 s photo etching indicate a V_{oc} of 0.60 V, J_{sc} of 7.50 mA cm^{-2}, ff of 0.53 and (of 3.0% for 80 mW cm^{-2} illumination. The photovoltaic parameters of the electrodes with and without photo etching is shown in Table 2. The efficiency of the photo electrodes is higher than the earlier reports [17–19].

Mott–Schottky plots ($1/C^2$ vs. V) were studied using 1 M Na_2SO_4 as the blocking electrolyte and an EG & G PARC impedance analyzer model 6310. The CdS films heat-treated at different temperatures were used as working electrode, graphite was used as counter electrode and SCE was used as the reference electrode. The frequency was fixed at 1 kHz and the bias voltage was varied in the range –0.8– + 0.4 V vs.

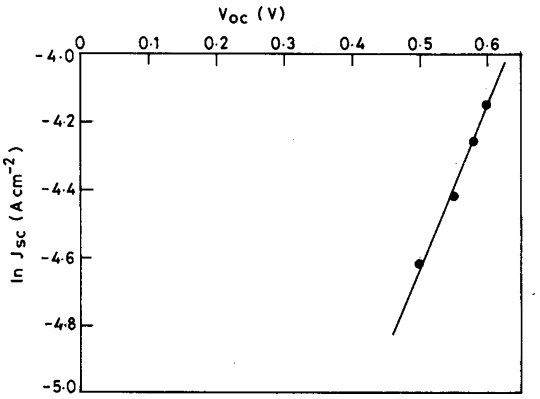

Fig. 7 Plot of lnJ_{sc} vs. V_{oc} of CdS photo electrodes heat treated in argon at 500 °C

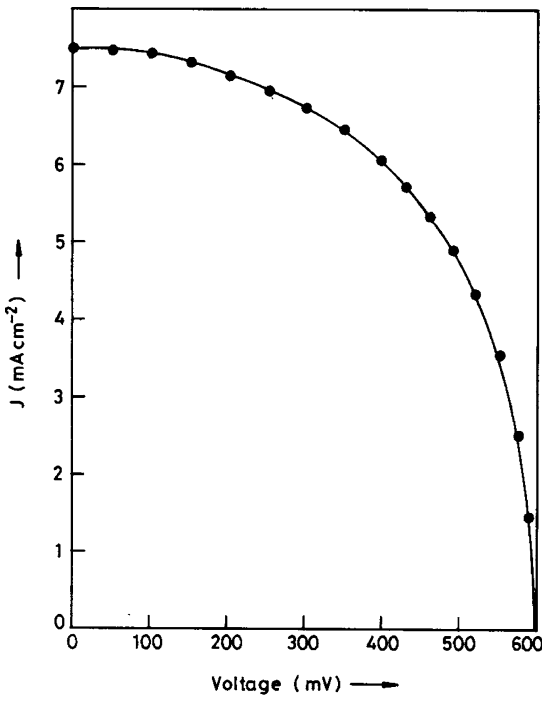

Fig. 9 Power output characteristics of CdS photoelctrodes heat treated in argon at 500 °C after photo etching for 80 s and illuminated at 60 mW cm^{-2}

Table 2 Photovoltaic parameters of CdS photoelectrodes (Intensity–80 Mw cm^{-2})

Temp of heat-treatment (°C)	V_{oc} (V)	J_{sc} (mA cm^{-2})	ff	(η%)	R_s (Ω)	R_{sh} (kΩ)
450	0.26	1.8	0.56	0.33	50.0	2.50
475	0.30	2.6	0.68	0.66	20.0	2.00
500	0.375	3.0	0.67	0.93	18.0	3.60
525	0.450	3.55	0.60	1.20	15.0	2.80
550	0.475	4.30	0.56	1.43	10.0	5.00
525 (After photo etch)	0.600	7.50	0.53	3.00	13.0	2.00

SCE, the value of C was estimated from the imaginary part of the impedance using the equation,

$$C = 1/2\,\pi\,fZ$$

Figure 10 exhibits the Mott–Schottky plots for the films heat-treated at different temperatures in the range 450–550°C. The nature of the plots indicates n-type behaviour. Extrapolation of the plot to the voltage axis yields a V_{fb} of –1.10 V (SCE). The value of carrier density from the slope of the plot yields a value around 2.0×10^{17} cm^{-3}. This value agrees well with the carrier density obtained from Hall measurements. The value of V_{fb} agrees well with the earlier reports [19].

Spectral response measurements were carried out on the photo electrodes by using photo physics monochromator and a 250 W tungsten halogen lamp, 1 M polysulphide as electrolyte, graphite as counter electrode and the photo electrode as the working electrode. The wavelength was varied in the range 400–900 nm and the photocurrent was noted at each wavelength.

The photocurrent value were used for the calculation of the quantum efficiency (ϕ) using the well known equation [20],

$$\Phi = 1240 J_{sc}/\lambda\, P_{in}$$

Where, J_{sc} is the photocurrent, λ is the wavelength of illumination, P_{in} is the power of the light incident on the photo electrode. Plot of ϕ versus λ for the CdS electrode heat treated at 500°C is shown in Fig. 11. The value of ϕ_{max} occurs at 0.525 μm corresponding to the band gap of 2.38 eV. This value matches well with the band gap value of 2.38 eV estimated from optical absorption measurements.

4 Conclusions

The results of this investigation indicate that the brush plating technique can be employed for the production of CdS films with ease and with small quantities of starting material compared to the conventional electrodeposition or chemical bath deposition methods. Moreover the process can be scaled up for the production of large area films to be used in photovoltaic devices. The efficiency could be further improved by doping the films with indium.

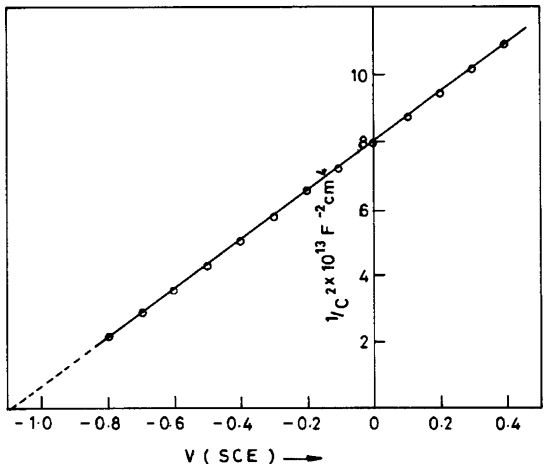

Fig. 10 Mott–Schottky plot of CdS photo electrodes heat-treated n argon at 500 °C

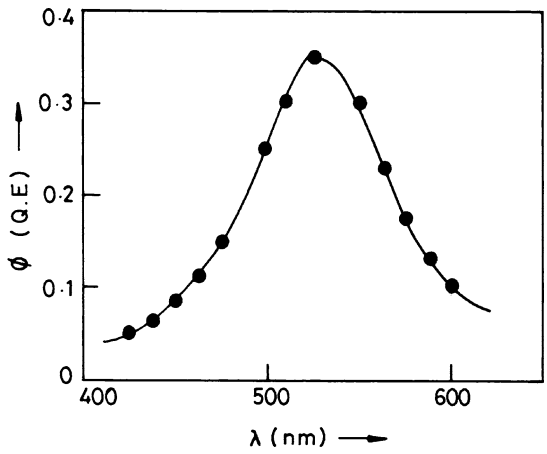

Fig. 11 Plot of ϕ vs. λ for the CdS electrode heat treated at 500°C

References

1. K. Senthil, D. Mangalaraj, S.K. Narayandass, Appl. Surf. Sci. **169–170**, 476 (2001)
2. G. Sasikala, P. Thilakan, C. Subramanian, Sol. Energy Mater. Sol. Cells **62**, 275 (2000)
3. A. Romeo, D.L. Bätzer, H. Zogg, C. Vignali, A.N. Tiwari, Sol. Energy Mater. Sol. Cells **67**, 311 (2001)
4. R. Inov, D. Desheva, Thin Solid Films. **213**, 230 (1992)
5. J. Pouzet, J.C. Bernede, A. Khellil, H. Essaidi, S. Benhida, Thin Solid Films. **208**, 252 (1992)
6. R.P. Raffaelle, H. Forsell, T. Potdevin, R. Fridefeld, J.G. Mantovani, S.G. Bailey, S.M. Hubbard, E.M. Gordon, A.F. Hepp, Sol. Energy Mater. Sol. Cells **57**, 167 (1999)
7. K. Subba Ramaiah, V. Sundara Raja, Sol. Energy Mater. Sol. Cells **32**, 1 (1994)
8. M.A. Contreras, M.J. Romero, B. To, F. Hasoon, R. Noufi, S. Ward, K. Ramanathan, Thin Solid Films **403–404**, 204 (2002)
9. K.R. Murali, V. Subramanian, N. Rangarajan, A.S. Lakshmanan, S.K. Rangarajan, J.Electroanal.chem. **368**, 95 (1994)
10. A. Cortez, H. Gomez, R.E. Marotti, G. Riveros, E.A. Dalchiele, Sol. Energy Mater Sol Cells **82**, 21 (2004)
11. C.M. Lampert, R. Mark, *Current Injection in solids*, Academic Press, NY, (1970)
12. K.R. Murali, I. Radhakrishna, K. Nagaraja Rao, V.K. Venkatesan, J.Mater.Sci. **25**, 3521 (1990)
13. R.K. Pandey, R.B. Gore, A.J.N. Rooz, J.Phys.D.Appl.Phys. **20**, 1059 (1987)
14. R.W. Smith, A. Rose, Phys.Rev. **97**, 1531 (1955)
15. R.H. Bube, A.L. Fahrenbruch, *Fundamentals of solar cells*, Academic Press (1983)
16. G. Hodes, Nature **285**, 29 (1980)
17. R.C. Bharadwaj, C.M. Jadhav, M.M. Taqui Khan, Sol.Cells **12**, 71 (1984)
18. M. Neumann Spallart, K. Kalyanasundaram, Ber.Bunsenges. Phys.Chem. **85**, 1112 (1981)
19. Y. Ramprakash, V. Subramanian, R. Krishnakumar, A.S. Lakshmanan, V.K. Venkatesan, J. Power sources **24**, 41 (1988)
20. J. Segui, S. Hot Chandani, D. Baddau, R.M. Leblanc, J. Phys. **94**, 8807 (1991)